RSC Advances

PAPER

View Article Online
View Journal | View Issue

Cite this: *RSC Adv.*, 2015, **5**, 1514

Phase behaviors of side chain liquid crystalline block copolymers

Xiaokang Li,[a] Feng Huang,[a] Tao Jiang,[a] Xiaohua He,[b] Shaoliang Lin*[a] and Jiaping Lin*[a]

Received 1st October 2014
Accepted 19th November 2014

DOI: 10.1039/c4ra11585f

www.rsc.org/advances

The microphase separation of side chain liquid crystalline (SCLC) block copolymers was studied using dissipative particle dynamics (DPD) simulations. The block copolymer monomer consists of flexible A segments and flexible B segments grafted by rigid C side chains, where the A, B and C blocks are incompatible with each other. The phase structures of the SCLC copolymers were found to be controlled by A and C block lengths and the graft number. Various mesophases, such as spheres, cylinders, gyroids, and lamellae, were obtained. Phase stability regions in the space of C block length and A block length (or graft number and A block length) were constructed. The packing ordering of C side chains was also studied, and discovered to increase as the temperature decreases or the rigid C side chains increase. In addition, the results of the SCLC copolymers were compared with those of flexible copolymers and available experimental observations. The simulation results in the present work provide useful information for future investigations on SCLC copolymers.

1. Introduction

In recent decades, the phase behaviors of block copolymers have attracted much attention, due to their promising applications in coatings and adhesive films.[1–6] The block copolymers can form classical microstructures, including lamellae, bicontinuous gyroids, hexagonally packed cylinders, and body-centered cubic spheres, as a consequence of microphase separation between different blocks.[7–11] So far, most of the block copolymers studied have been flexible copolymers. In contrast with flexible block copolymers, block copolymers containing rigid segments (liquid crystalline copolymers) can form nanostructures with higher degrees of ordering, since the rigid segments can lead to orientation organization.[12–16] When the rigid segments act as side chains grafted on a polymer backbone, a side chain liquid crystalline (SCLC) block copolymer is obtained. The SCLC copolymers possess the characteristics of both graft copolymers and liquid crystalline copolymers, which may make them useful for applications in the fields of biomedicine and nanotechnology.[17–21]

Experimentally, the SCLC block copolymers have been widely applied to prepare a variety of ordered nanostructures.[22–33] The phase behaviors of SCLC block copolymers are very complicated, due to the coexistence of microphase separation and the orientation of rigid segments in packing.[26–34] de Wit and co-workers reported the phase behavior of poly(4-vinylpyridine) (P4VP)-based azobenzene-containing copolymers, as investigated by DSC and simultaneous SAXS/WAXS.[26] They found that the SCLC copolymers tend to form the lamellar phase and exhibit smectic ordering in the azobenzene domain. Korhonen *et al.* synthesized a series of SCLC block copolymers through attaching rigid cholesteryl hemisuccinate (CholHS) to flexible poly(styrene)-*b*-poly(4-vinylpyridine) (PS-*b*-P4VP) block copolymers.[34] The SCLC copolymers can self-assemble into hierarchical structures, in which the smectic layers of CholHS are perpendicular to the block domain interface. However, due to the structural complexities of SCLC copolymers and the limitations of experimental technology, many important issues, including the mechanisms by which chain packing and external factors influence the phase behavior, are little understood.

In addition to experimental observations, theories and computer simulations have emerged as powerful tools to study the phase behaviors of complex polymers.[35–43] They can provide more straightforward results than pure experiments, and overcome the limitations inherent in experiments. So far, various approaches, such as self-consistent field theory (SCFT),[35,36] Monte Carlo (MC) simulations,[37] molecular dynamics (MD) simulations,[38] and dissipative particle dynamics (DPD) simulations,[39,40] have been widely employed to investigate the phase behaviors of flexible block and graft copolymers. However, theoretical and simulation studies on the phase behavior of SCLC block copolymers are very limited.[41–43] For example, Shah and co-workers proposed a SCFT model and a strong segregation theory (SST) based analytical theory to understand the thermodynamic behavior of SCLC block copolymers.[41] The SCLC copolymer can phase separate into lamellar and cylindrical phases with rigid blocks in dispersed or continuous

[a]*Shanghai Key Laboratory of Advanced Polymeric Materials, Key Laboratory for Ultrafine Materials of Ministry of Education, School of Materials Science and Engineering, East China University of Science and Technology, Shanghai 200237, China. E-mail: slin@ecust.edu.cn; jlin@ecust.edu.cn; Tel: +86-21-6425-1011*

[b]*Department of Chemistry, East China Normal University, Shanghai 200241, China*

domains. In the lamellae, the orientation direction of the rigid side chains is parallel to the block copolymer interface, while in the cylinders it is parallel to the long axis of the cylinders. Stimson *et al.* carried out MD simulations on the phase structures of polysiloxane SCLC block copolymers.[43] The SCLC copolymers self-organize into lamellar phases with polymer-rich and mesogen-rich regions, as the systems are cooled from fully isotropic polymer melts. Within the smectic phases, the backbone was perpendicular to the directors of smectic-A. Compared with SCFT and MD simulations, DPD simulation can access greater lengths and time scales, and thus predominates in the study of the phase behaviors of polymers. However, to the best of our knowledge, no studies on the phase behavior of SCLC block copolymers using the DPD method have been reported. Many issues remain to be solved in the complex system, and the microphase separation of SCLC block copolymers needs to be explored further. Understanding the principles of phase separation and chain packing will facilitate the preparation of novel nanostructures and applications in advanced materials.

In the present work, we performed a dissipative particle dynamics simulation to study the phase behaviors of SCLC block copolymers, which consist of flexible A blocks, flexible B blocks grafted by rigid C side chains. The effects of A and C block lengths, and the graft number, on the phase structures were examined. Stability regions of various mesophases were constructed in the space of the C block length and A block length (or graft number and A block length). The packing ordering of the rigid C side chains was also studied. Additionally, a comparison of the phase behaviors between SCLC block copolymers and flexible copolymers was made. The simulation results were also compared with the available experimental observations.

2. Method and model

2.1 Simulation method

Dissipative particle dynamics was first proposed by Hoogerbrugge and Koelman,[44,45] and is suitable for complex fluids.[46–48] It is a combination of molecular dynamics, lattice-gas automata, and Langevin dynamics, which obeys Galilean invariance, isotropy, mass conservation, and momentum conservation. In the method, a bead having mass m represents a block or cluster of atoms or molecules moving together in a coherent fashion. The DPD beads are subject to soft potentials and governed by predefined collision rules.[49]

In the method, the force $\mathbf{f}_i$ acting on bead i is a pairwise additive force, consisting of the conservative force ($\mathbf{F}_{ij}^{C}$), dissipative force ($\mathbf{F}_{ij}^{D}$), and random force ($\mathbf{F}_{ij}^{R}$), given by[48]

$$\mathbf{f}_i = \sum_{j \neq i} \left(\mathbf{F}_{ij}^{C} + \mathbf{F}_{ij}^{D} + \mathbf{F}_{ij}^{R} \right) \quad (1)$$

The conservative force is a soft repulsion taking the following form:

$$\mathbf{F}_{ij}^{C} = a_{ij} \sqrt{\omega(r_{ij})}\, \hat{\mathbf{r}}_{ij} \quad (2)$$

where a_{ij} is the maximum repulsive interaction between beads i and j, $\mathbf{r}_{ij} = \mathbf{r}_i - \mathbf{r}_j$, $r_{ij} = |\mathbf{r}_{ij}|$, $\hat{\mathbf{r}}_{ij} = \mathbf{r}_{ij}/r_{ij}$, and $\omega(r_{ij})$ is the weight function given by

$$\omega(r_{ij}) = \begin{cases} (1 - r_{ij}/r_c)^2 & (r_{ij} < r_c) \\ 0 & (r_{ij} \geq r_c) \end{cases} \quad (3)$$

according to the study by Groot and Warren, and r_c is the cutoff radius ($r_c = 1.0$). The dissipative force is a frictional force that acts on the relative velocities of beads, defined by

$$\mathbf{F}_{ij}^{D} = -\gamma \omega^{D}(r_{ij})(\hat{\mathbf{r}}_{ij} \cdot \mathbf{v}_{ij})\hat{\mathbf{r}}_{ij} \quad (4)$$

and the random force, compensating the loss of kinetic energy due to the dissipative force, is defined by

$$\mathbf{F}_{ij}^{R} = \sigma \omega^{R}(r_{ij})\theta_{ij}\hat{\mathbf{r}}_{ij} \quad (5)$$

where $\mathbf{v}_{ij} = \mathbf{v}_i - \mathbf{v}_j$, γ is the friction coefficient, σ is the noise amplitude, $\omega^{D}(r_{ij})$ and $\omega^{R}(r_{ij})$ are weight functions vanishing for $r > r_c$ that describe the range of the dissipative and random forces, and θ_{ij} is a randomly fluctuating variable with Gaussian statistics:

$$\langle \theta_{ij}(t) \rangle = 0,\ \langle \theta_{ij}(t)\theta_{kl}(t') \rangle = (\delta_{ik}\delta_{jl} + \delta_{il}\delta_{jk})\delta(t - t') \quad (6)$$

In order to satisfy the fluctuation-dissipation theorem and for the system to evolve to an equilibrium state that corresponds to the Gibbs canonical ensemble, only one of $\omega^{D}(r_{ij})$ and $\omega^{R}(r_{ij})$ can be chosen arbitrarily and the other one is then fixed by the relation[47,48]

$$\omega^{D}(r_{ij}) = [\omega^{R}(r_{ij})]^2 = \omega(r_{ij}) \quad (7)$$

and the values of parameters γ and σ are coupled by

$$\sigma^2 = 2\gamma k_B T \quad (8)$$

where T is the absolute temperature, and k_B is the Boltzmann constant.

For the copolymers, the interaction force between bonded beads is considered as a harmonic spring force,

$$\mathbf{F}_{ij}^{S} = C(1 - r_{ij}/r_{eq})\hat{\mathbf{r}}_{ij} \quad (9)$$

where C is the spring constant and r_{eq} is the equilibrium bond distance. In order to reinforce the rigidity of the side chains, one angle force is added between every two consecutive bonds. The bond angle θ is constrained as 180°, and the angle force is defined by

$$\mathbf{F}^{A} = -\nabla[k_\theta(\theta - \pi)^2] \quad (10)$$

where k_θ is the angle constant. The larger the k_θ value, the more rigid the side chains.

In the DPD method, reduced units are adopted for all physical quantities.[48] The units of mass, length, time, and

energy are defined by m, r_c, τ, and k_BT, respectively. The time unit τ can be formulated by

$$\tau = \sqrt{(mr_c^2)/k_BT} \quad (11)$$

and its real value can be estimated by matching the simulated lateral diffusion coefficient to the experimental measured value.

2.2 Model and conditions

In the simulation, we constructed a coarse-grained model of SCLC block copolymers, with the typical structure shown in Fig. 1. The copolymer consists of a flexible A block with x beads and a flexible B block with y beads that is grafted by n rigid C chains with z beads on each chain. The block copolymers are denoted by A_x-b-(B_y-g-nC_z), where b and g are short for "block" and "graft", respectively. In the expression, $y = 2n$, therefore, the total bead number N in one copolymer molecule satisfies: $N = x + n(z + 2)$. Note that this model can represent varieties of analogous SCLC copolymers that possess characteristics of microphase separation and LC ordering, such as the block copolymer containing a flexible P4VP block and the rigid side chains of azobenzene moieties.[34,50]

All the simulations were carried in a cubic box ($30 \times 30 \times 30$) with periodic boundary conditions adopting the NVT ensemble. The temperature T was set to 1.0, except for when studying the temperature effect. The friction coefficient γ, noise amplitude σ, and number density ρ were set to 4.5, 3.0, and 3.0, respectively. The time step was set as $\Delta t = 0.02\tau$. The spring constant C and equilibrium bond distance r_{eq} were chosen as 100 and 0.8. A larger angle constant k_θ of 200 was set to ensure the rigidity of C side chains. The interaction between identical species was set to be 25, while the interaction parameters between different species were all fixed at 60, implying that the different species are incompatible. To capture the equilibrated structures, 2.0×10^6 DPD steps were carried out. When studying the ordered packing of rigid chains, we annealed the system from $T = 1.0$ to $T = 0.1$ during 1.8×10^7 DPD steps.

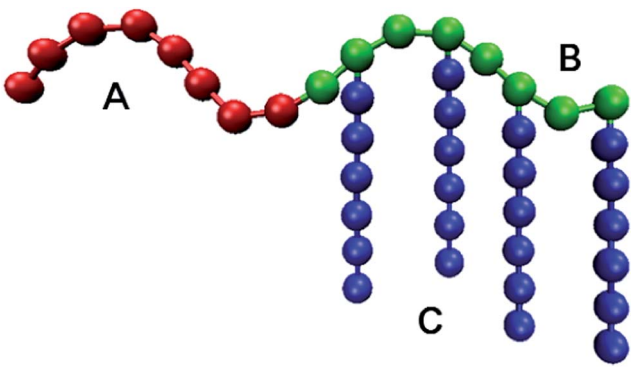

Fig. 1 Coarse-grained model for the SCLC block copolymers. The beads colored red, green, and blue represent flexible A block, flexible B block, and rigid C side chains, respectively.

3. Results and discussion

In this work, three-component SCLC block copolymers were applied to form diverse mesophases in melt. The molecular architecture, including block length, graft number and temperature, are important parameters governing the phase behaviors of SCLC copolymers. The lengths of the A, B, and C blocks are denoted by the bead numbers of blocks in one polymer chain, *i.e.*, $x = N_A$, $y = N_B$, and $z = N_C$. In what follows, the influence of these parameters, designated N_A, N_C, n and T, was examined in particular. The simulation of the similar A_x-b-(B_y-g-nC_z), in which the C blocks were made flexible, was additionally carried out, in order to explore the influence of the rigidity of the side chains.

3.1 Influence of block lengths and graft number on phase behavior

In this subsection, the investigation of the phase behaviors of SCLC block copolymers as a function of A block length N_A, C block length N_C, and graft number n is described. The N_A was varied from 4 to 100, while N_C was changed from 5 to 8. And the block copolymers with graft number $n = 2$, 3, 4 and 5 were considered. For various values of n, the B block length N_B should be chosen according to the relation $y = 2n$. All phase structures were equilibrated at temperature $T = 1.0$, corresponding to a melt state.

We first considered the model of a SCLC block copolymer with $N_B = 8$, $N_C = 6$, and $n = 4$. Fig. 2 shows the self-assembly structures observed at various lengths (N_A) of A blocks. As can be seen from Fig. 2a, the SCLC block copolymers form a spherical structure (S_A) when the A block length is smaller ($N_A = 4$). The A spheres surrounded by B blocks are dispersed in a matrix of C blocks. When N_A increases to 8, the block copolymers phase-separate into a cylindrical structure (C_A), where the cylinders of A blocks covered by B blocks are hexagonally aligned in the matrix of C blocks (Fig. 2b). When N_A is 24, a gyroid phase (G_A) in which the minority domains of B-covered A blocks and a continuous matrix of C blocks are observed (see Fig. 2c). When N_A is further increased, a lamellar structure (L) is produced at $N_A = 48$, which contains one thick A lamella and three thin BCB lamellae, as shown in Fig. 2d. Fig. 2e shows a gyroid structure (G_C) with the B-covered C blocks forming the minority domains in the A matrix at $N_A = 80$. It is apparent from Fig. 2 that the ordered phase transitions of $S_A \rightarrow C_A \rightarrow G_A \rightarrow L \rightarrow G_C$ occur as N_A increases. The phase transition can be explained as follows. When the A blocks are short, the A blocks occupy the minor domains, forming phases such as S_A and C_A. As the lengths of the A blocks increase, the chains become stretched in the minor domains, and the conformation entropy becomes unfavorable. To relax the A blocks, L and G_C are formed. In these structures, the A blocks occupy the major domains. Through the phase transitions, the conformation entropy arising from chain stretching becomes favorable. However, the interfacial/surface energy increases.

Subsequently, the effect of C block length N_C was examined. Combining the effects of N_A and N_C, the thermodynamic

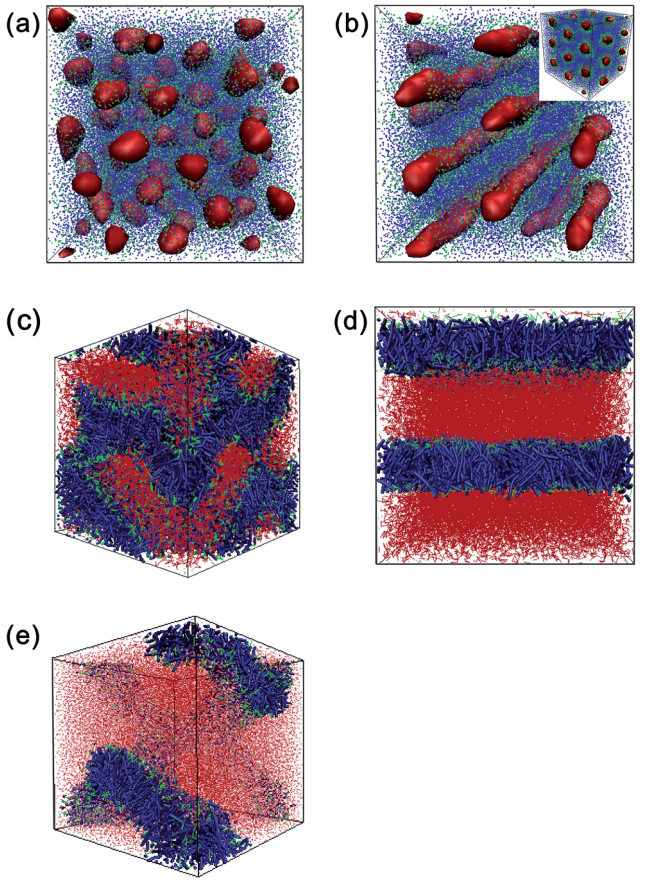

Fig. 2 Simulated structures formed by SCLC block copolymers with $N_B = 8$, $N_C = 6$, and $n = 4$: (a) spheres, S_A, (b) cylinders, C_A, (c) gyroids, G_A, (d) lamellae, L, and (e) gyroids, G_C. The subscripts A and C in S, C, and G denote that the minority domains of the ordered structures are formed by A and C blocks, respectively. From (a) to (e), the lengths of A blocks (N_A) are 4, 8, 24, 48, and 80, respectively. The red, green, and blue colors are assigned to A, B, and C blocks, respectively.

stability regions of phase-separated structures were constructed. Fig. 3 presents the phase stability regions in the space of N_C *vs.* N_A for SCLC block copolymers with $N_B = 8$ and $n = 4$. The mesophases include S_A, C_A, G_A, L, and G_C. It can be found that with increasing N_C, the C_A and L regions become narrower and wider, respectively, while the width of the G_A region stays roughly unchanged. Note that when the N_C increases to 7, the S_A phase disappears, and the C_A phase also disappears when N_C is 8. The formation of spherical and cylindrical structures is unfavourable with longer C side chains. The boundaries of the C_A and L regions tend to shift toward a smaller N_A, while the left and right boundaries of the G_A region move to a smaller N_A and a larger N_A, respectively. It suggests that at a constant N_A the lamellae form more easily than spheres, cylinders, and gyroids for longer C blocks.

In Fig. 3, the lamellar phase occupies a wider region at a larger N_C. With increasing N_C, the stretching action of A blocks decreases while the orientation of C blocks takes over the greater function. To maintain the system stability, the lamellar structure is a preferable structure and the lamellar region is

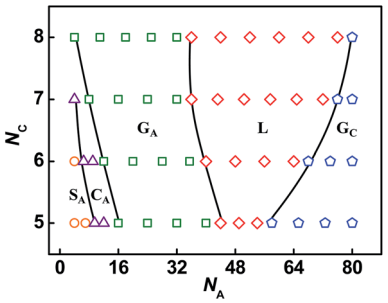

Fig. 3 Phase stability regions of SCLC block copolymers in the space of N_C *vs.* N_A. The ordered regions are denoted as S (spheres), C (hexagonally packed cylinders), G (bicontinuous gyroids), and L (lamellae). The subscripts A and C in S, C, and G indicate that the minority domains of the ordered structures are formed by A and C blocks, respectively. The B block length N_B is fixed as 8, and the graft number n is 4. Regions of S_A (○), C_A (△), G_A (□), L (◇), and G_C (⬠) phases are shown.

broadened at a higher N_C. At higher N_A, the phase transition of $G_C \rightarrow L$ appears as N_C increases. As the rigid C blocks become longer, the blocks are orientated to reduce the loss of orientation entropy. Thus, in L phases, the rigid C blocks can be packed in an entropically favorable manner compared with in the G_C phases. On the other hand, the interfacial/surface energy becomes unfavorable.[53,54] Additionally, at a constant N_C, as the N_A increases, the phase transition experiences the progress of $S_A \rightarrow C_A \rightarrow G_A \rightarrow L \rightarrow G_C$. Originally, the volume fraction of A blocks was too low, so that C blocks were inclined to form the matrix and the S_A, C_A and G_A phases are formed. When N_A was large enough, the lamellar phase was generated, with the interaction of A blocks and C blocks. Further increasing the N_A value, the volume fraction of the LC component was low, so that the orientation of the C block had only a slight effect. Therefore, the L phase was transformed into the G_C phase.

In addition to the block length, the effect of the graft number n on the phase behavior was also studied. The phase stability regions in the space of n *vs.* N_A are shown in Fig. 4, where the C block length N_C was set to be 6. At $n = 2$ and 3, no S_A and C_A phases were formed. As the n increased, the C_A, G_A, and L regions became wider. The boundaries of the C_A, G_A, and L regions all moved to a larger N_A, which is different from the

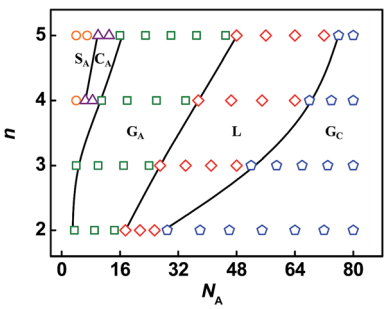

Fig. 4 Phase stability regions in the space of n *vs.* N_A for SCLC block copolymers with $N_C = 6$. Regions of S_A (○), C_A (△), G_A (□), L (◇), and G_C (⬠) phases are shown.

effect of N_C. The SCLC block copolymers tended to form the G_C phase at a lower n but form the L or G_A phase at a higher n at a constant N_A. It can be seen in Fig. 4 that the graft number n markedly influenced the phase structures of the SCLC block copolymers. As the graft number increased, the volume fraction of the LC component increased, while the volume fraction of the A blocks decreased. Similar to the discussion above, the increasing of the LC component was favorable for packing ordering, resulting in the lamellar phase occupying a wider region at a larger value of n. Overall, the formation of different phase structures can be speculated to be a balance of stretching and orientation from A blocks and C blocks separately.

3.2 Influence of temperature on the packing ordering of rigid C side chains

In this subsection, the investigation of the packing ordering of rigid C side chains in various ordered structures is described. The orientation degree was characterized by the order parameter S, which is an average value of order parameter S_i of the i-th rigid chain. The S_i is defined by $S_i = \frac{3(\mathbf{u}_i \cdot \mathbf{u}_d)^2 - 1}{2}$, where $\mathbf{u}_i$ is the normalized vector of the i-th rigid chain, $\mathbf{u}_d$ is the normalized vector of orientation direction, which is determined by iteration to find the maximum value of S_i by dividing the polar-coordinate space into pieces. First, we studied the effect of temperature on the chain packing state in several typical structures through annealing the systems from a higher temperature ($T = 1.0$) to a lower temperature ($T = 0.1$). Then we calculated the order parameter S as a function of temperature at various values of N_A and N_C.

Three typical structures, *i.e.* the C_A, L, and G_C phases, were taken as examples. Fig. 5 presents the structures formed by SCLC block copolymers at various values of N_A when the temperature was reduced to 0.1. We mainly focused on the packing of the rigid C side chains. As shown in Fig. 5a, a cylindrical structure (C_A) is formed at $N_A = 8$, in which the C chains are packed in an orderly manner and perpendicularly to the long axes of the cylinders consisting of A blocks covered by B blocks. Fig. 5b shows a lamellar structure with the C chains parallel with each other at $N_A = 56$. The highly orientated packing of rigid chains was achieved at a lower temperature, and the lamellar structure is a smectic-like structure. At $N_A = 80$, the gyroid structure (G_C), with B-covered C blocks forming the minority domains in the A matrix, indicates that the rigid C chains are aligned with each other in a twisting manner, as shown in Fig. 5c. It is concluded from Fig. 5 that rigid chains can be packed more regularly when the temperature is decreased to a lower value.

In order to further understand the influence of temperature on the packing ordering of rigid C chains, the order parameters of C chains in a lamellar structure were explored at various temperatures. The results at $N_A = 48$ are shown in Fig. 6. The insert shows the typical simulation snapshots at various temperatures. At $T = 1.0$, the order parameter S is low and an unordered lamella was obtained. As the temperature decreases, the S increases gradually, and finally reaches a plateau. The S is about 0.75 when T is decreased to 0.2, indicating that the rigid chains are orientated and packed regularly in the lamellar domains. A smectic-like structure is formed gradually as the system temperature is decreased. The result implies that the temperature has marked influences on the packing ordering of rigid chains.[55,56]

Subsequently, to study the effect of the lengths of the A and C blocks on chain packing ordering, the S values of C side chains as a function of temperature at various values of N_C and N_A were calculated, where only the lamellar phase was considered. Fig. 7a shows the order parameter S at temperatures ranging from 1.0 to 0.1 for block copolymers with $N_C = 5$, 6, 7, and 8. The other parameters are $N_A = 56$, $N_B = 8$, and $n = 4$. As can be seen, for any N_C the S exhibits the same trend of increasing with a decrease in temperature. At a fixed temperature, the effect of N_C can be seen. The S has a higher value at a larger N_C, indicating

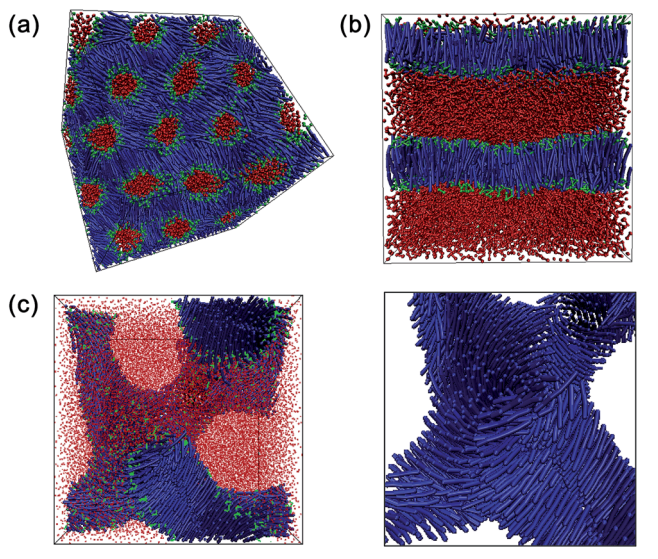

Fig. 5 Typical structures formed by SCLC block copolymers at various values of N_A when the temperature was decreased to 0.1: (a) cylindrical structure (C_A) at $N_A = 8$, (b) lamellar structure (L) at $N_A = 56$, and (c) gyroid structure (G_C) at $N_A = 80$. In figure (c), the local packing of the C side chains is also shown.

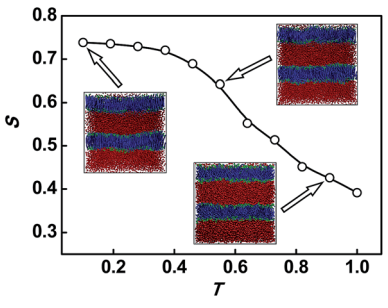

Fig. 6 Variation of the order parameter S of the rigid C side chains in a lamellar structure as a function of the system temperature T. The lamellae are formed by block copolymers with $N_A = 48$, $N_B = 8$, $N_C = 6$, and $n = 4$. The inset shows the typical simulation snapshots at various values of T.

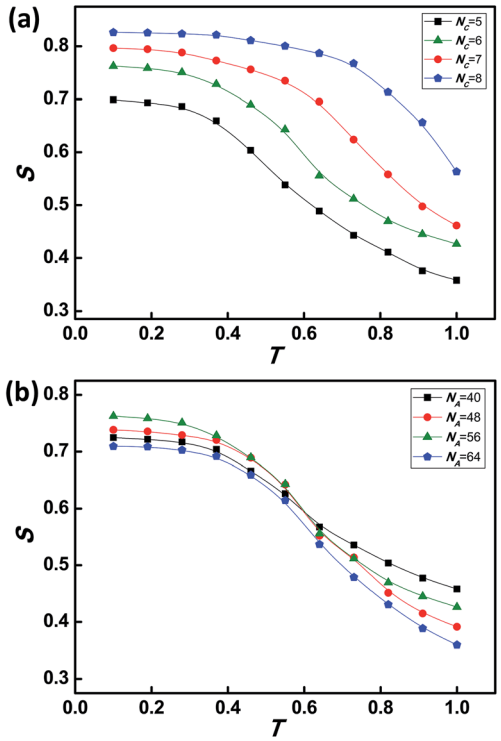

Fig. 7 Variation of the order parameter S of the C chains as a function of temperature for SCLC block copolymers (a) with various values of N_C, and (b) with various values of N_A. In part (a), the N_C was changed from 5 to 8, and the other parameters were $N_A = 56$, $N_B = 8$, and $n = 4$. In figure (b), the N_A was varied from 40 to 64, while N_B, N_C, and n were fixed as 8, 6, and 4, respectively.

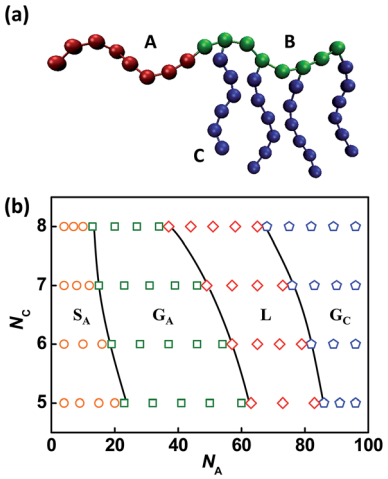

Fig. 8 (a) The flexible block copolymer similar to the SCLC copolymer, with the exception of coiled side chains. (b) Phase stability regions of flexible block copolymers in the space of N_C *vs.* N_A at $T = 1.0$. The regions of S_A, G_A, L, and G_C phases are obtained. The B block length N_B is fixed at 8, and the graft number n is 4.

that longer C chains can benefit their ordered packing. On the other hand, the S values *versus* temperature at various values of N_A are presented in Fig. 7b. The N_A was varied from 40 to 64, while N_B, N_C, and n were fixed as 8, 6, and 4, respectively. It shows that at various values of N_A, S has a similar trend with an increase in temperature (discussed above). However, the N_A was discovered to have a slight influence on the S values. From Fig. 7, we can see that the length of the rigid C side chains is crucial to chain packing ordering relative to the length of flexible A chains, and the A block length mainly influences the phase regions.

3.3 Comparison with flexible copolymers and available experimental observations

In this subsection, the comparison of the phase behaviors of flexible block copolymers and SCLC block copolymers is described. As can be seen in Fig. 8a, the flexible block copolymer possesses the same molecular structure, except that the side chains become coiled rather than rigid. The block components and interaction parameters of the flexible copolymers were chosen to be the same as those of the SCLC copolymers. This can benefit our understanding of the effect of introducing rigid side chains on the phase behaviors of three-component block copolymers. Through adjusting the lengths of the C and A blocks, the phase stability regions in the space of N_C and N_A were also constructed. Then we compared the simulation results of the SCLC copolymers and available experimental observations.

Fig. 8b shows the phase stability regions in the space of N_C *vs.* N_A for flexible block copolymers with $N_B = 8$ and $n = 4$ at $T = 1.0$. The value of N_A was varied from 4 to 80, while N_C was changed from 5 to 8. Similar to the SCLC block copolymers, S_A, G_A, L, and G_C regions were obtained. However, under the parameter conditions employed, cylindrical structures could not be observed, and the C_A region was absent. Relative to the SCLC block copolymers, we could also find that the G_A region became broader while the L region was narrower for flexible block copolymers. The lamellar structures were generated at a larger N_A, and the boundary between the G_A and L regions moved to a larger N_A. This suggests that the introduction of rigid side chains is favorable for the formation of lamellar structures at a smaller N_A. Besides the diversity in the phase boundaries, the ordering of the chain packing is also different for flexible and SCLC copolymers. In flexible copolymers, the chains are unable to orient as rigid blocks and are thereby positioned irregularly. During microphase separation, the flexible chains are stretched to accommodate the structures, while the rigid blocks change their orientations to adjust the structures.

Recently, some experimental observations regarding the SCLC copolymers became available in the literature that support our predictions.[50–52,57] Mao *et al.* synthesized a series of SCLC block copolymers by attaching azobenzene mesogenic groups to the isoprene block of polystyrene-*b*-poly(1,2-&-3,4-isoprene) (PS-*b*-PI) block copolymers *via* acid chloride coupling.[50] The bulk structures of the SCLC block copolymers were studied and found to be controlled by the volume fraction of the LC component. The coil cylinders formed at a higher LC volume fraction were transformed into a lamellar structure and then into a bicontinuous structure, with minority domains of

the LC component, as the LC volume fraction decreases. Anthamatten and co-workers also found that the SCLC block copolymers of polystyrene and methacrylates containing (*s*)-2-methyl-1-butyl-4′-(((4-hydroxyphenyl)carbonyl)oxy)-1,1′-biphenyl-4-carboxylate mesogens (PS-*b*-HBPB) can form hexagonally close-packed PS cylinders at a higher LC volume fraction, while they self-assemble into completely lamellar structures or predominantly lamellar structures at a lower LC volume fraction.[51,52] These experimental observations are in qualitative accordance with the simulated phase transition from C_A to L and then to G_C with an increasing value of N_A.

M. Yamada and co-workers prepared a kind of SCLC copolymer containing a polystyrene segment and a 6-[4-(4-methoxyphenyl)phenoxy]-hexyl methacrylate (MPPHM) segment,[57] which is similar to our model, as the MPPHM segment can be divided into a B block and C block. These copolymers exhibited a well-defined lamellar type of segregation, and the side chain LC segments formed the smectic A crystalline phase and isotropic arrangements with an increase in temperature. This tendency coincides well with our finding that the order parameter increases with a decrease in temperature (see Fig. 6 and 7). Whilst there are similarities, some differences were also observed. For example, in our simulations, a G_A structure with the coil blocks forming the minority domains was predicted, but this was not found in the experiments. This difference may result from the coarse-grained model in the DPD simulations and the limited samples in the experiments. In addition, our predictions also reveal the mechanism of the phase transition, which may provide guidance for further studies of phase structures of SCLC block copolymers.

In this work, the phase behaviors of SCLC block copolymers were investigated by the DPD method for the first time. Various ordered nanostructures were formed, including hexagonally packed cylinders seldom observed in existing reports, and the morphological window of this category of copolymers was further expanded. The structural parameters of the SCLC copolymers, including the block length and graft number, were found to play important roles in determining the phase structures. In addition, the simulations provide chain packing information that cannot be obtained in experiments. The simulation results could be helpful for developing promising strategies to control the complex structures formed by SCLC copolymers.

4. Conclusions

In this work, we have investigated the phase behavior of SCLC block copolymers using DPD simulations. It was found that the S_A, C_A, G_A, L, and G_C phases are formed sequentially as the N_A increases. Moreover, with an increasing value of N_C or n, lamellar phases with extensive regions were formed. The thermodynamic stability regions of these phases were constructed by combining these two effects, *i.e.*, N_C *vs.* N_A and n *vs.* N_A. The phase transitions are a balance of interaction enthalpy and the entropy resulting from the stretching of flexible A/B chains and the orientation of rigid C chains. On reducing the temperature, the order parameters of the C blocks increased and the packing of rigid C side chains exhibited higher ordering. Compared with flexible copolymers, the regions of L phases were enlarged and the boundary between the G_A and L regions moved to a lower N_A for the SCLC copolymers. In addition, a general agreement with experimental observations was found, but with some differences. The differences may result from the coarse-grained model in the DPD simulations and the limited samples in experiments. The present work could be of guiding significance for understanding the phase behavior of SCLC block copolymers.

Acknowledgements

This work was supported by National Natural Science Foundation of China (51103044, 21174038 and 50925308). Support from Projects of Shanghai Municipality (11QA1401600, 13ZZ041 and 12JC1403102) and Fundamental Research Funds for the Central Universities (20100074120001, NCET-12-0857 and WD1213002) is also appreciated.

References

1 R. Resendes, J. A. Massey, H. Dorn, K. N. Power, M. A. Winnik and I. Manners, *Angew. Chem., Int. Ed.*, 1999, **38**, 2570–2573.
2 W. van Zoelena and G. ten Brinke, *Soft Matter*, 2009, **5**, 1568–1582.
3 Z. Li, E. Kesselman, Y. Talmon, M. A. Hillmyer and T. P. Lodge, *Science*, 2004, **306**, 98–101.
4 D.-G. Kim, H. Kang, S. Han, H. J. Kima and J.-C. Lee, *RSC Adv.*, 2013, **3**, 18071–18081.
5 H. Otsukaa, Y. Nagasakib and K. Kataoka, *Curr. Opin. Colloid Interface Sci.*, 2001, **6**, 3–10.
6 Z. Wang, G. Wen, F. Zhao, C. Huang, X. Wang, T. Shi and H. Li, *RSC Adv.*, 2014, **4**, 29595–29603.
7 V. Percec, C. H. Ahn and G. Ungar, *Nature*, 1998, **391**, 161–164.
8 S. B. Darling, *Prog. Polym. Sci.*, 2007, **32**, 1152–1204.
9 M. W. Matsen and F. S. Bates, *Macromolecules*, 1996, **29**, 7641–7644.
10 J. Chatterjee, S. Jain and F. S. Bates, *Macromolecules*, 2007, **40**, 2882–2896.
11 R. Nagarajan and K. Ganesh, *J. Chem. Phys.*, 1989, **90**, 5843–5856.
12 S. A. Jenekhe and X. L. Chen, *Science*, 1999, **283**, 372–375.
13 S. A. Jenekhe and X. L. Chen, *Science*, 1998, **279**, 1903–1907.
14 T. Kato, *Science*, 2002, **295**, 2414–2418.
15 S.-C. Tsao and C.-T. Lo, *RSC Adv.*, 2014, **4**, 23585–23594.
16 J.-G. Lia and S.-W. Kuo, *RSC Adv.*, 2011, **1**, 1822–1833.
17 W. Sun, X. He, X. Liao, S. Lin, W. Huang and M. Xie, *J. Appl. Polym. Sci.*, 2013, **130**, 2165–2175.
18 P. Fatás, J. Bachl, S. Oehm, A. I. Jiménez, C. Cativiela and D. D. Díaz, *Chem.–Eur. J.*, 2013, **19**, 8861–8874.
19 K. Gayathrt, S. Balamurugan and P. Kannan, *J. Chem. Sci.*, 2011, **123**, 255–263.
20 O. Ikkala and G. ten Brinke, *Chem. Commun.*, 2004, 2131–2137.
21 G. ten Brinke and O. Ikkala, *Chem. Rec.*, 2004, **4**, 219–230.

22 H. Fischer and S. Poser, *Acta Polym.*, 1996, **47**, 413–428.
23 R. P. Nieuwhof, A. T. M. Marcelis, E. J. R. Sudholter, S. J. Picken and W. H. de Jeu, *Macromolecules*, 1999, **32**, 1398–1406.
24 A. Laiho, P. Hiekkataipale, J. Ruokolainen and O. Ikkala, *Macromol. Chem. Phys.*, 2009, **210**, 1218–1223.
25 A. J. Soininen, I. Tanionou, N. ten Brummelhuis, H. Schlaad, N. Hadjichristidis, O. Ikkala, J. Raula, R. Mezzenga and J. Ruokolainen, *Macromolecules*, 2012, **45**, 7091–7097.
26 J. de Wit, G. A. van Ekenstein, E. Polushkin, K. Kvashnina, W. Bras, O. Ikkala and G. ten Brinke, *Macromolecules*, 2008, **41**, 4200–4204.
27 S. Lin, Y. Wang, C. Cai, Y. Xing, J. Lin, T. Cheng and X. He, *Nanotechnology*, 2013, **24**, 085602.
28 Y. Wang, S. Lin, M. Zang, Y. Xing, X. He, J. Lin and T. Chen, *Soft Matter*, 2012, **8**, 3131–3138.
29 A. Martínez-Felipe, C. T. Imrie and A. Ribes-Greus, *Ind. Eng. Chem. Res.*, 2013, **52**, 8714–8721.
30 E. Barmatov, *Macromolecules*, 2002, **35**, 3076–3082.
31 A. Kozak, J. J. Moura-Ramos, G. P. Simon and G. Williams, *Macromol. Chem. Phys.*, 1989, **190**, 2463–2476.
32 S. Chen, A. Ling and H.-L. Zhang, *J. Polym. Sci., Part A: Polym. Chem.*, 2013, **51**, 2759–2768.
33 S. H. Goh, Y. H. Lai and S. X. Cheng, *Liq. Cryst.*, 2001, **28**, 1527–1538.
34 J. T. Korhonen, T. Verho, P. Rannou and O. Ikkala, *Macromolecules*, 2010, **43**, 1507–1514.
35 L. Wang, J. Lin and L. Zhang, *Langmuir*, 2009, **25**, 4735–4742.
36 L. Wang, T. Jiang and J. Lin, *RSC Adv.*, 2013, **3**, 19481–19491.
37 M. Kenward and M. D. Whitmore, *J. Chem. Phys.*, 2002, **116**, 3455–3470.
38 M. Mondeshki, G. Mihov, R. Graf, H. W. Spiess and K. Müllen, *Macromolecules*, 2006, **39**, 9605–9613.
39 T. Jiang, L. Wang and J. Lin, *RSC Adv.*, 2014, **4**, 35272–35283.
40 T. Jiang, L. Wang, S. Lin, J. Lin and Y. Li, *Langmuir*, 2011, **27**, 6440–6448.
41 M. Shah, V. Pryamitsyn and V. Ganesan, *Macromolecules*, 2008, **41**, 218–229.
42 M. Anthamatten and P. T. Hammond, *J. Polym. Sci., Part B: Polym. Phys.*, 2001, **39**, 2671–2691.
43 L. M. Stimson and M. R. Wilson, *J. Chem. Phys.*, 2005, **123**, 034908.
44 P. J. Hoogerbrugge and J. M. V. A. Koelman, *Europhys. Lett.*, 1992, **19**, 155–160.
45 J. M. V. A. Koelman and P. J. Hoogerbrugge, *Europhys. Lett.*, 1993, **21**, 363–368.
46 Y. Xu, J. Feng and H. Liu, *Mol. Simul.*, 2008, **34**, 559–565.
47 P. Espanol and P. B. Warren, *Europhys. Lett.*, 1995, **30**, 191–196.
48 R. D. Groot and P. B. Warren, *J. Chem. Phys.*, 1997, **107**, 4423–4435.
49 Y.-J. Sheng, C.-H. Nung and H.-K. Tsao, *J. Phys. Chem. B*, 2006, **110**, 21643–21650.
50 G. Mao, J. Wang, S. R. Clingman and C. K. Ober, *Macromolecules*, 1997, **30**, 2556–2567.
51 M. Anthamatten and P. T. Hammond, *Macromolecules*, 1999, **32**, 8066–8076.
52 W. Y. Zheng and P. T. Hammond, *Macromolecules*, 1998, **31**, 711–721.
53 K. Gordon, B. Sannigrahi, P. Mcgeady, X. Q. Wang, J. Mendenhall and I. M. Khan, *J. Biomater. Sci., Polym. Ed.*, 2009, **20**, 2055–2072.
54 S. T. Milner, *Science*, 1991, **251**, 905–914.
55 A. AlSunaidi, W. K. den Otter and J. H. R. Clarke, *Philos. Trans. R. Soc., A*, 2004, **362**, 1773–1781.
56 A. AlSunaidi, W. K. den Otter and J. H. R. Clarke, *J. Chem. Phys.*, 2009, **130**, 124910.
57 M. Yamada, T. Iguchi, A. Hirao, S. Nakahama and J. Watanabe, *Polym. J.*, 1998, **30**, 23–30.